scientific reports

Check for updates

OPEN

Rescattering effects in the reaction $\gamma d \to \pi^- pp$

Vyacheslav Gauzshtein[1,2]✉, Eed Darwish[3,4], Darya Efimenko[2], Alexander Fix[1,2], Vladislav Ivanov[1], Michael Levchuk[5,6], Alexey Loginov[2,7], Dmitry Nikolenko[1], Igor Rachek[1], Yuriy Shestakov[1,8], Dmitry Toporkov[1], Bogdan Vasilishin[2], Arseniy Yurchenko[1], Sergey Zevakov[1], Grigoriy Baranov[1], Anton Bogomyagkov[1], Vladislav Borin[1], Darya Dorokhova[1], Victor Dorokhov[1], Andrey Zhuravlev[1], Kseniya Karyukina[1], Artemiy Kovalenko[1], Vasiliy Kudryavtsev[1], Evgeniy Levichev[1], Ivan Logashenko[1], Timofey Maltsev[1], Rasim Mamutov[1], Ivan Morozov[1], Ivan Okunev[1], Pavel Piminov[1], Lev Shekhtman[1], Evgeniy Simonov[1], Sergey Sinyatkin[1], Mikhail Skamarokha[1], Elena Starostina[1], Ivan Ulev[1] & Hoda Abou-Elsebaa[3,4]

Experimental data for the tensor analyzing power T_{20} in the $\gamma d \to \pi^- pp$ reaction were obtained in the photon energy range from 400 to 650 MeV, with the proton momenta in the laboratory system exceeding 400 MeV/c. The data were taken at the Budker Institute of Nuclear Physics using an internal tensor-polarized gas deuterium target and tagged photons. The incident photons in the photoproduction reaction $\gamma d \to \pi^- pp$ correspond to quasi-real virtual photons generated via electron scattering in the electroproduction process $ed \to e\pi^- pp$ at small four-momentum transfer. The two final protons were detected in coincidence. The tensor analyzing power T_{20} was extracted from the yield asymmetry observed upon reversal of the sign of the deuteron tensor polarization. The experimental results are compared with statistical simulations performed within the framework of a spectator model that includes interaction between the final particles. The comparison demonstrates that accounting for the interaction effects significantly improves the agreement with the data.

Keywords Photonuclear reactions, Polarization phenomena in reactions, Spin observables, Few-body systems, Forces inhadronic systems and effective interactions

Using photomeson reactions to study the structure of hadronic systems offers several significant advantages. First, the electromagnetic photon–nucleon interaction is well described within the framework of hadron electrodynamics. Second, at the large momentum transfers, characteristic of these reactions, virtual photons scan a nucleus at short distances, which allows one to obtain more complete information about nuclear interaction.

Photomeson reactions also enable the investigation of the structure of excited baryon states, particularly their excitation spectra and electromagnetic transition form factors. This bridges functional approaches in quantum chromodynamics with methods based on effective field theories and connects directly to a wealth of existing experimental studies[1,2]. Experiments particularly well suited for these purposes are the quasi-free production studies on light nuclei, primarily the deuteron. Due to its low binding energy and well-understood structure, the deuteron serves as an effective laboratory for investigating various aspects of meson-nucleon dynamics in electromagnetic reactions under controlled conditions.

Despite these advantages, the interpretation of the corresponding experimental results often depends on the theoretical model employed to describe the reaction. The main reason is that QCD, the fundamental theory of the strong interaction, cannot be treated perturbatively at low energies. This forces us to apply various approaches based on effective field theory, lattice QCD, chiral perturbation theory, non-relativistic scattering theory, and constituent quark model[2–6]. Being inherently phenomenological, these theoretical frameworks typically have limited predictive power. Consequently, different models often yield similar results only for a

[1]Budker Institute of Nuclear Physics, Novosibirsk, Russia630090. [2]National Research Tomsk Polytechnical University, Tomsk, Russia634050. [3]Physics Department, College of Science, Taibah University, 41411 Medina, Saudi Arabia. [4]Physics Department, Faculty of Science, Sohag University, Sohag 82524, Egypt. [5]Stepanov Institute of Physics, National Academy of Sciences of Belarus, 220072 Minsk, Belarus. [6]Institute of Applied Physics, National Academy of Sciences of Belarus, 220072 Minsk, Belarus. [7]Tomsk State University of Control Systems and Radioelectronics, Tomsk, Russia634050. [8]Novosibirsk State University, Novosibirsk, Russia630090. ✉email: V.V.Gauzshteyn@inp.nsk.su

restricted set of observables, most notably the unpolarized differential cross section, while their predictions for other observables may differ significantly. Therefore, to assess the validity and applicability of various model approaches, it is essential to measure as broad a set of independent observables as possible.

In the present paper, we study the incoherent photoproduction of negative pions on the deuteron

$$\gamma + d \to \pi^- + p + p. \tag{1}$$

In the intermediate photon energy region ($E_\gamma < 1$ GeV), this reaction is well described within the impulse approximation, which leads to the so-called spectator model. In this framework, the pion is assumed to be produced on a single quasi-free (active) nucleon, while the second nucleon acts as a spectator and does not participate in the interaction. This model has been widely employed in the literature (see, e.g.,[7–9] and references therein) and provides a reliable first approximation, capturing the dominant dynamical features of the reaction, at least in kinematic regions close to the quasi-free maximum.

The most important corrections to the quasi-free mechanism arise from final state interaction (FSI), specifically, *NN* and πN rescatterings. These additional mechanisms can significantly affect the energy and angular distributions of the outgoing particles and must therefore be included in any realistic description. Moreover, FSI in pion photoproduction is of intrinsic interest: the πNN system constitutes the simplest three-body system in which one of the particles, the pion, can be emitted or absorbed. In this sense, the dynamics of this system lies between that of nonrelativistic scattering theory and full quantum field theory. Consequently, the consistent inclusion of FSI effects in pion photoproduction on deuterons represents an important challenge in intermediate-energy pion-nuclear physics. This has motivated numerous theoretical studies aimed at identifying observables that are particularly sensitive to FSI, thereby allowing their effects to be clearly isolated and quantified.

One may expect FSI effects to be particularly significant in cases where the primary mechanism, photoproduction on quasi-free nucleons, is suppressed. This is precisely the situation in the kinematic region under study, where the average momenta p of the outgoing nucleons significantly exceed the characteristic momentum in the deuteron, $p_0 = \sqrt{M\varepsilon_d} \approx 45$ MeV/c with ε_d denoting the deuteron binding energy and M the nucleon mass. The FSI mechanism enables the transferred momentum to be shared between both nucleons, thereby compensating for the imbalance between p and p_0 and thus effectively reducing the aforementioned suppression.

In the case of polarization observables, FSI effects are further enhanced, as measurements involving polarized particles are generally more sensitive to various corrections than unpolarized cross sections. In particular, studies such as[8,10] have shown that for the reaction $\gamma d \to \pi^- pp$, the tensor analyzing power components, T_{20}, T_{21}, and T_{22}, exhibit significant sensitivity to *NN* and πN rescattering effects. Moreover, theoretical predictions indicate that the rescattering contribution increases with both the momentum transfer to the deuteron and the relative momentum of the final-state nucleon pair.

Setting up experiments to measure tensor asymmetries in photo-reactions on the deuteron requires a tensor polarized deuterium target. However, a high degree of tensor polarization can be achieved only with gaseous deuterium. This requirement severely limits the target thickness and thereby reduces the luminosity of experiments performed with an extracted electron beam, rendering their implementation practically unfeasible. For this reason, experimental studies of tensor asymmetries have never been included in the research programs of leading facilities such as ELSA[11], MAMI[12], JLab[13], and ELPH[14]. Nevertheless, such experiments can be carried out without significant loss of luminosity by employing the internal target method. In this approach, an ultra-thin gaseous deuterium target is placed directly inside the accelerator ring, enabling operation without electron beam extraction and thus avoiding beam current loss. The high circulating beam current compensates for the reduced target density, allowing luminosities comparable to those achieved with solid targets. This technique was pioneered at the Budker Institute of Nuclear Physics in the mid-1960s with the development of the first electron storage rings and is currently implemented at the VEPP-3 accelerator facility[15].

Over the past 30 years, a number of experiments have been carried out at VEPP-3 to measure tensor asymmetries for various photoreactions on a deuteron. In particular, accurate experimental values of the T_{20}, T_{21}, and T_{22} components of the tensor analyzing power have been obtained in the photodisintegration channel, $\gamma d \to pn$, in Ref.[16]. In addition, the energy and angular dependencies of T_{20} for the reaction $\gamma d \to \pi^0 d$ have been measured in[17–20], where strong discrepancy between the experimental data and theoretical predictions was noted in the region of large momentum transfer[21]. As for study of the reaction (1) at VEPP-3, the first results for tensor asymmetry were obtained from the statistics accumulated in 1999[22] and 2002–2003[23]. At the same time, due to the low statistical accuracy, these results allowed only a qualitative comparison with the existing theoretical predictions.

The first precise results for T_{20} in the reaction (1) were obtained in 2021 for the photon energies in the range $300 \le E_\gamma \le 500$ MeV[24]. A comparative analysis based on sophisticated model calculations demonstrated that including *NN* and πN rescattering significantly improves the agreement between data and theory. At the same time, at higher energies ($E_\gamma > 500$ MeV), where the typical momentum transfers increase, rescattering effects are expected to become even more pronounced.

Therefore, to achieve better conditions for studying the FSI effects, it is reasonable to move to higher energies. A possibility to measure the tensor asymmetry for the reaction $\gamma d \to \pi^- pp$ at $E_\gamma > 500$ MeV appeared only in 2023 due to the commissioning of the photon tagging system at VEPP-3. The first preliminary results for T_{20} in the photon energy range 400–650 MeV were obtained in 2023 and published in[25]. Here, we present our final results and provide a detailed analysis of the role of rescattering in the large momentum transfer regime.

Research method

The basis of the polarization experiments at VEPP-3 is the measurement of the asymmetry in the reaction yield with respect to the sign reversal of the tensor polarization of the deuterium target. The experimental setup comprises a detection system for reaction products, a photon tagging system (PTS), an internal target cell, a source of polarized deuterium atoms, and a Low-Q Polarimeter (LQP). Except for the detection system and the PTS, all components have undergone only minor modifications over the past 20 years.

The design of the detection system is determined by the kinematic parameters and the types of particles to be detected. In particular, in 2012, a deuteron (or proton) in coincidence with one or two gamma quanta from the decay of a neutral pion was registered, enabling reconstruction of the kinematics of the two processes: $\gamma d \to \pi^0 d$ and $\gamma d \to \pi^0 pn$. During 2002–2003, coincidence data were accumulated for proton–neutron and proton–proton events, which allowed extraction of information on deuteron photodisintegration and incoherent pion photoproduction on the deuteron.

The results presented in the present paper were obtained from the experimental statistics accumulated in 2023. The corresponding experimental setup is shown in Fig. 1. The detection system is designed to register proton–neutron and proton-proton coincidences. Protons were detected by the drift chambers (DC) and the scintillation spectrometers in the range of the polar emission angle 50°–90° and the kinetic energy 55–170 MeV.

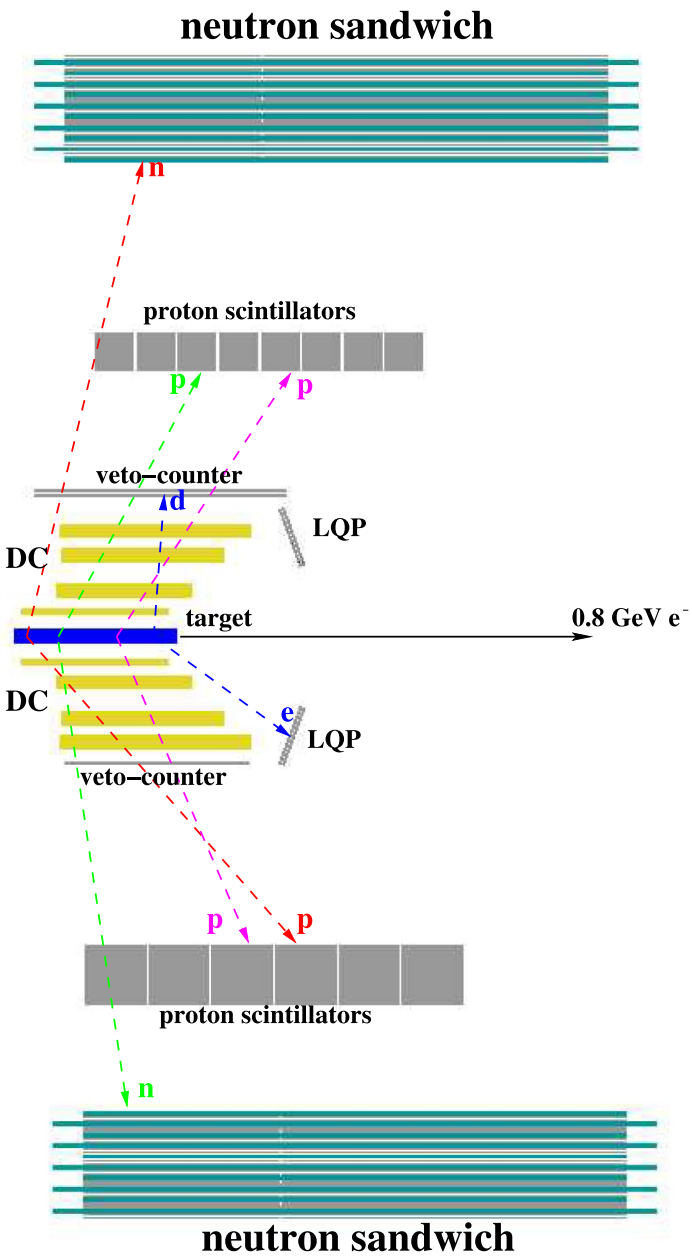

Fig. 1. Experimental scheme.

Neutrons were recorded by sectional sandwich calorimeters consisting of ten layers of iron and scintillation strips. To extract $\gamma d \to \pi^- pp$ events, the statistics corresponding to proton–proton coincidences was used.

For proton identification, the veto counter and proton scintillators are used in each arm. In the upper arm, identification is based on the $\Delta E/E$ analysis, while in the lower arm, the *TOF*/*E* method is applied. In both detection arms, the kinetic energy of protons is reconstructed from the energy deposited in the proton scintillators. For energy calibration, GEANT4 simulations were employed. To select $\gamma d \to \pi^- pp$ events, the pion mass was reconstructed using the measured proton kinematic parameters together with the photon energy recorded by PTS. To validate the event selection procedure, the results of the data analysis were compared with those obtained from GEANT4 simulations using the GENBOS photoreaction generator[26]. The GENBOS generator was developed at JLab and is used for simulating photoreactions on the deuteron. GEANT4 simulations incorporating GENBOS were also employed to estimate the number of irreducible background events. A detailed description of the proton detection procedure, identification of the $\gamma d \to \pi^- pp$ reaction, and assessment of the background are presented in Ref.[25].

The photon tagging system is a new component at VEPP-3, first commissioned in 2023. Its distinctive feature is that it must operate with the electron beam inside the acceleration chamber. This significantly complicates both the operational principle and the mechanical design of the PTS compared to those at JLab[27] or MAMI[28]. The reason is that, unlike the single-dipole-magnet photon tagging systems employed at external-target facilities such as JLab and MAMI, the PTS at VEPP-3 requires the installation of three precisely aligned dipole magnets, a set of synchrotron radiation absorbers, and a compact tracking system within the limited space of the VEPP-3 straight section.

The PTS operation schematic is shown in Fig. 2. At the first stage, the electron beam is deflected from the initial orbit by the first dipole magnet D1 and directed onto the internal target. After passing through the target, the electrons enter the second dipole magnet, which, together with the GEM trackers, functions as a magnetic spectrometer, measuring the energy of scattered electrons in the range $0.2E_0$ to $0.5E_0$, where E_0 is the beam energy. Thus, the energy range of the tagged photons is $(0.5–0.8)E_0$. In particular, for an electron beam with an energy of 800 MeV, the tagged photons are registered in the range 400–650 MeV. Electrons that have not undergone an interaction with the target are returned to the initial orbit by the third dipole magnet D3. For a detailed description of the PTS at VEPP-3, we refer the reader to Ref.[29].

The tensor-polarized deuterium target is an elliptical storage cell built into the accelerating ring. During the experiment, gaseous tensor-polarized deuterium from the source of polarized atoms[30] was continuously fed into the cell. At the output of the polarized atom source, the tensor polarization is close to 100%, and its sign is flipped every 30 s (from -2 to $+1$).

Inside the storage cell, however, the tensor polarization is significantly reduced due to various depolarizing effects. Therefore, its degree within the storage cell is continuously monitored during data acquisition. For this purpose, the experimental setup is supplemented with an LQP, whose operating principle is based on measuring the asymmetry in elastic *ed* scattering at small momentum transfer.

To register the *ed* coincidences, an electron detector was mounted, and part of the main detector was used to detect the recoil deuterons. In the present work, the thin veto counters of the upper arm of the detection system were employed to detect the recoil deuterons (see Fig. 1). More information about the LQP can be found in Ref.[31].

The tensor polarization P_{zz} of the deuteron target may be expressed in terms of the populations $n_{0,\pm1}$ of the deuteron states with the spin projections $s_z = 0, \pm 1$ on the direction of the magnetic field as

$$P_{zz} = 1 - 3n_0 = 3(n_+ + n_-) - 2. \tag{2}$$

During the experiment, the deuteron target could be in the state with a positive (negative) tensor polarization P_{zz}^+ (P_{zz}^-). According to the LQP data, the degree of tensor polarization averaged over the full duration of the experiment was $P_{zz}^+ = 0.39 \pm 0.025 \pm 0.009$ and $P_{zz}^- = -0.66 \pm 0.043 \pm 0.015$, where the first and the second uncertainties are statistical and systematic, respectively.

We denote by N^+ (N^-) the number of the reaction events corresponding to the tensor polarization P_{zz}^+ (P_{zz}^-) of the deuteron target and registered in a given kinematic region. The experimental setup described above has

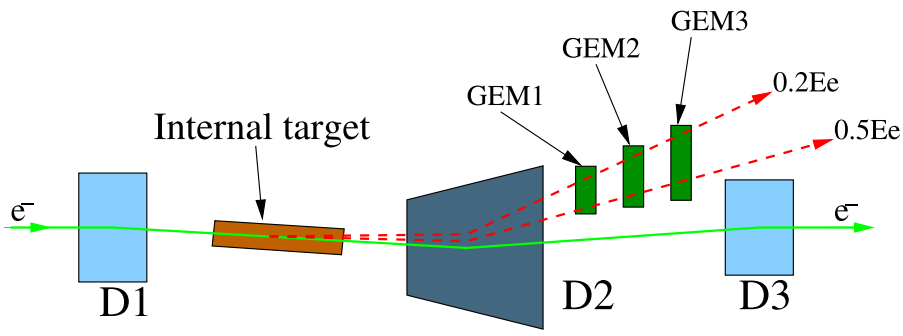

Fig. 2. The photon tagging system, top view. D1, D2, D3: dipole magnets, GEM1, GEM2, GEM3: tracking detectors.

allowed us to measure the asymmetry $A^T = N^+ - N^-$ of the reaction yield with respect to the change of the sign of the tensor polarization P_{zz}. To suppress possible systematic error in measuring A^T, the sign of P_{zz} was reversed every 30 s. In the general case, however, all the three components T_{20}, T_{21}, and T_{22} of the tensor analyzing power contribute to A^T.

To extract an individual component T_{2M}, one should use the general expression for the differential cross-section,

$$d\sigma = d\sigma_0 \left\{ 1 + \frac{1}{\sqrt{2}} P_{zz} \left[d^2_{00}(\theta_H)\, T_{20} - d^2_{10}(\theta_H) \cos(\phi_H)\, T_{21} + d^2_{20}(\theta_H) \cos(2\phi_H)\, T_{22} \right] \right\}, \tag{3}$$

where $d\sigma$ ($d\sigma_0$) is the polarized (unpolarized) differential cross-section, $d^j_{mm'}(\theta_H)$ are the Wigner rotation matrices defined as in[32], and the angles θ_H and ϕ_H determine the orientation of the magnetic field in the coordinate system with the z axis directed along the photon momentum. Note, that Eq. (3) refers to the coplanar kinematics when the momenta of all the three final particles lie in the same plane in the laboratory system.

In the present experiment, the magnetic field was directed along the photon beam, so that the angle $\theta_H = 0$. In this case, only the term with T_{20} survives in the square brackets in Eq. (3). Taking into account that the number of registered events $N^{\pm}$ in a given kinematic region is proportional to the corresponding differential cross-section (3), one obtains

$$N^{\pm} = N_0 \left\{ 1 + \frac{1}{\sqrt{2}} P^{\pm}_{zz} T_{20} \right\}, \tag{4}$$

where N_0 is the number of reaction events in the unpolarized case. Equation (4) directly yields the expression for the T_{20} component in terms of the experimentally measured quantities:

$$T_{20} = \sqrt{2}\, \frac{N^+ - N^-}{P^+_{zz} N^- - P^-_{zz} N^+}. \tag{5}$$

Results

Our data are presented in Fig. 3. On the left panel, the dependence of T_{20} on the proton–proton invariant mass $M_{pp} = (4m_p^2 + p_r^2)^{1/2}$ is shown, where p_r is the magnitude of the relative pp momentum of the proton pair in the center-of-mass frame, and m_p is the proton mass. On the right panel, T_{20} is presented as a function of the momentum p_s, defined as the smaller of the momenta of the two final protons in the laboratory frame. Statistical and systematic uncertainties are shown together with the experimental points. The dominant source of the systematic uncertainty is the uncertainty in the degree of the deuteron tensor polarization and the contribution from irreducible background events.

In addition to the experimental points, Fig. 3 presents the results of Monte Carlo simulations. The reaction amplitude used in the simulation algorithm was calculated within the model of Ref.[33], which includes the

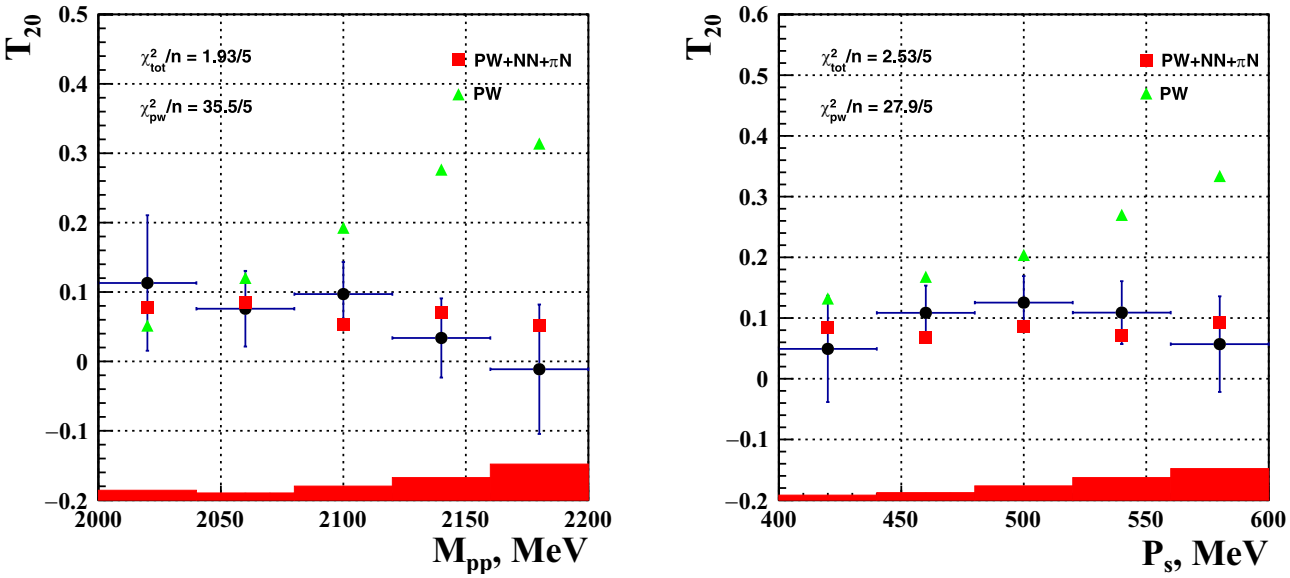

Fig. 3. The tensor analyzing power component T_{20} for the reaction $\gamma d \to \pi^- pp$ as a function of the proton-proton invariant mass M_{pp} (left panel) and the momentum of the slow proton (right panel). The black filled circles represent the experimental results. Statistical and systematic uncertainties (red lines at the bottom) are shown together with the data points. The red squares (green triangles) correspond to the results of simulations based on the spectator model with (without) inclusion of πN and NN rescattering in the final state.

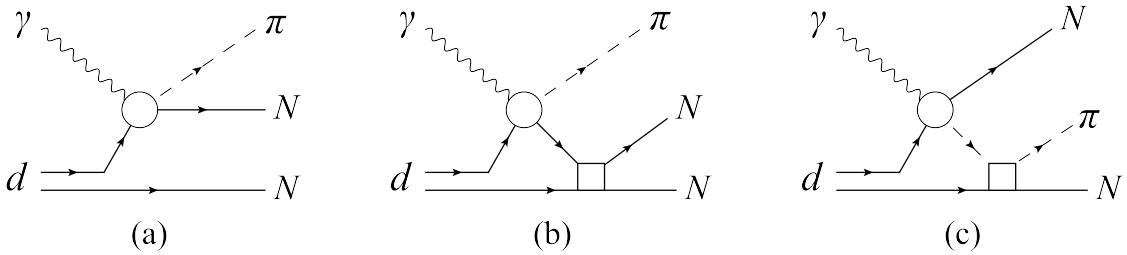

Fig. 4. The mechanisms of the incoherent pion photoproduction on a deuteron: (**a**) quasi-free pion photoproduction on a single nucleon, (**b**) *NN* rescattering, (**c**) πN rescattering.

contributions of the three diagrams shown in Fig. 4. Among the FSI mechanisms, *NN* rescattering turns out to be particularly important, primarily due to the significantly higher intensity of the *NN* interaction compared to πN (see also the discussion in Refs.[7–9]). Furthermore, in our experiment both final protons have relatively high kinetic energies, and the *NN* rescattering mechanism efficiently redistributes energy between the fast active nucleon and the spectator. In contrast, the intermediate pion cannot transfer a sufficient amount of kinetic energy between the two nucleons because of its small mass. The Monte Carlo simulation was performed using the algorithm described in detail in Ref.[34]. The energy of the incident photons was sampled according to the Dalitz spectrum[35].

As may be seen from Fig. 3, the tensor analyzing power T_{20} is rather small in the kinematic region under consideration. It is also evident that the experimental results cannot be satisfactorily described, if a pure spectator model that neglects FSI is used. The discrepancy increases with the relative momentum of the proton pair. In contrast, inclusion of rescattering effects significantly improves the agreement with the data, particularly in the region of large relative proton–proton momentum. The overall agreement between experiment and simulation is fairly good ($\chi^2_{tot}/n < 1$).

One may anticipate that a possible future improvement of experimental data may necessitate a refinement of the theory, in particular, the incorporation of additional mechanisms into the model. Such mechanisms might include, for example, the interaction between a single nucleon and a nucleon resonance in an intermediate state, or the contribution of the $\Delta\Delta$ component of the deuteron wave function[36,37]. Higher-order multiple-scattering diagrams[38] may also play a role in the kinematic region of the present experiment.

In this regard, we would like to highlight an aspect of the $\gamma d \to \pi NN$ processes that is generally little discussed in the literature. Namely, in the first and second resonance regions, a rather strong discrepancy persists between theory and experiment[8], especially in the $\pi^0 np$ channel, the origin of which is still not very well understood. One commonly considered explanation is that certain additional FSI mechanisms are still missing from current models. This may be particularly relevant in the second resonance region, where various inelastic channels ($K\Lambda$, $\pi\pi N$, etc.) start to open. However, our analysis strongly suggests that the source of the present discrepancy apparently lies elsewhere, possibly in the very mechanism of pion photoproduction on a quasi-free nucleon itself.

Conclusion

We have obtained new, relatively precise data for the tensor analyzing power T_{20} in the reaction $\gamma d \to \pi^- pp$ in the photon energy range from 400 to 650 MeV and for proton momenta $p_{1,2} > 400$ MeV/c. The kinematic region considered in the present analysis is of particular interest due to its enhanced sensitivity to final state interaction effects. The measured values of T_{20} were compared with the results of Monte Carlo simulations performed within the framework of a spectator model that also includes FSI mechanisms (*NN* and πN rescattering in the final state).

The dependence of T_{20} on the final particle energies shown in Fig. 3 constitutes the most informative aspect of our measurement and, within the context of the presented analysis, represents our main result. By comparing the Monte Carlo calculations with the experimental data, we conclude that the overall structure of the T_{20} energy spectra is reasonably well described, indicating that our interpretation of the reaction mechanism is essentially correct. The agreement between the calculated and measured values is rather good, especially considering the high sensitivity of polarization observables to the details of the wave function and the *NN* and πN scattering amplitudes. The calculations successfully reproduce the deviation of the experimental T_{20} values from the predictions of the pure spectator model, demonstrating that this deviation is primarily attributable to FSI.

Overall, our results clearly demonstrate that FSI effects become appreciable in the kinematic region under study and tend to grow with increasing final proton momentum as well as with increasing invariant mass of the final *pp*-system. Their inclusion significantly improves the agreement between theory and experiment.

Data availability

The datasets generated during and/or analysed during the current study are available from the corresponding author on reasonable request.

Received: 17 September 2025; Accepted: 24 December 2025
Published online: 03 January 2026

References

1. Eichmann, G., Sanchis-Alepuz, H., Williams, R., Alkofer, R. & Fischer, C. S. Baryons as relativistic three-quark bound states. *Prog. Part. Nucl. Phys.***91**, 1. https://doi.org/10.1016/j.ppnp.2016.07.001 (2016).
2. Döring, M., Haidenbauer, J., Mai, M. & Sato, T. Dynamical coupled-channel models for hadron dynamics. *Prog. Part. Nucl. Phys.***146**, 104213. https://doi.org/10.1016/j.ppnp.2025.104213 (2026).
3. Thiel, A., Afzal, F. & Wunderlich, Y. Light baryon spectroscopy. *Prog. Part. Nucl. Phys.***125**, 103949. https://doi.org/10.1016/j.ppnp.2022.103949 (2022).
4. Mai, M., Meißner, U.-G. & Urbach, C. Towards a theory of hadron resonances. *Phys. Rept.***1001**, 1. https://doi.org/10.1016/j.physrep.2022.11.005 (2023).
5. Meißner, U.-G. & Bernard, V. Chiral perturbation theory. *Annu. Rev. Nucl. Part. Sci.***57**, 33. https://doi.org/10.1146/annurev.nucl.56.080805.140449 (2023).
6. Diakonov, D. Foundations of the constitutent quark model. *Prog. Part. Nucl. Phys.***36**, 1. https://doi.org/10.1016/0146-6410(96)00003-8 (1996).
7. Laget, J. Electromagnetic properties of the πNN-system. the reaction $\gamma D \to NN\pi$. *Nucl. Phys. A***296**, 388. https://doi.org/10.1016/0375-9474(78)90081-7 (1978).
8. Fix, A. & Arenhöevel, H. Incoherent pion photoproduction on the deuteron with polarization observables influence of final state rescattering. *Phys. Rev. C***72**, 064005. https://doi.org/10.1103/PhysRevC.72.064005 (2005).
9. Levchuk, M. I., Loginov, A. Y., Sidorov, A. A., Stibunov, V. N. & Schumacher, M. Incoherent pion photoproduction on the deuteron in the first resonance region. *Phys. Rev. C***74**, 014004. https://doi.org/10.1103/PhysRevC.74.014004 (2006).
10. Briscoe, W. J., Kudryavtsev, A. E., Strakovsky, I. I., Tarasov, V. E. & Workman, R. On the photoproduction reactions $\gamma d \to \pi NN$. *Eur. Phys. J. A***58**, 23. https://doi.org/10.1140/epja/s10050-022-00671-4 (2022).
11. Seifen, T. et al. Polarization observables in double neutral pion photoproduction. *Eur. Phys. J. A***61**, 173. https://doi.org/10.1140/epja/s10050-025-01612-7 (2025).
12. Bashkanov, M. et al. Deuteron photodisintegration by polarized photons in the region of the $d^*(2380)$. *Phys. Let. B***789**, 7. https://doi.org/10.1016/j.physletb.2018.12.026 (2019).
13. Skorodumina, I. et al. Double-pion electroproduction off protons in deuterium: Quasifree cross sections and final-state interactions. *Phys. Rev. C***109**, 065205. https://doi.org/10.1103/PhysRevC.109.065205 (2024).
14. Ishikawa, T. et al. First measurement of coherent double neutral-pion photoproduction on the deuteron at incident energies below 0.9 gev. *Phys. Lett. B***772**, 398. https://doi.org/10.1016/j.physletb.2017.04.010 (2017).
15. Budker, G., Onuchin, A., Popov, S. & Tumaikin, G. Experiments with target in electron storage ring. *Phys. Atom. Nucl.***6**, 775 (1967).
16. Rachek, I. et al. Measurement of tensor analyzing powers in deuteron photodisintegration. *Phys. Rev. Lett.***98**, 182303. https://doi.org/10.1103/PhysRevLett.98.182303 (2007).
17. Zevakov, S. et al. Neutral pion photoproduction on tensor-polarized deuterium on the VEPP-3 storage ring. *Bull. Russ. Acad. Sci. Phys.***78**, 611. https://doi.org/10.3103/S1062873814070260 (2014).
18. Zevakov, S. et al. Measuring tensor analyzing power component t_{20} of the coherent photoproduction of a neutral pion on a tensor-polarized deuteron in the VEPP-3 storage ring. *Bull. Russ. Acad. Sci. Phys.***79**, 864. https://doi.org/10.3103/S1062873815070266 (2015).
19. Rachek, I. et al. Measurement of tensor analyzing power t_{20} in coherent π^0 photoproduction on deuteron. *Few-Body Syst.***58**, 29. https://doi.org/10.1007/s00601-016-1191-0 (2017).
20. Gauzshtein, V. et al. Measurement of the tensor analyzing power t_{20} for the reaction $\gamma d \to d\pi^0$. *Eur. Phys. J. A***56**, 169. https://doi.org/10.1140/epja/s10050-020-00175-z (2020).
21. Gauzshtein, V. et al. Coherent photoproduction of a π^0-meson on a tensor-polarized deuteron at large momentum transfer. *Results Phys.***38**, 105573. https://doi.org/10.1016/j.rinp.2022.105573 (2022).
22. Barkov, L. et al. Tensor asymmetry of π^0-meson photoproduction on polarized deuterons. *Bull. Russ. Acad. Sci. Phys.***74**, 743. https://doi.org/10.3103/S1062873810060031 (2010).
23. Gauzshtein, V. et al. Measurement of tensor analyzing powers of the incoherent pion photoproduction on a deuteron. *Nucl. Phys. A***968**, 23. https://doi.org/10.1016/j.nuclphysa.2017.07.019 (2017).
24. Gauzshtein, V. et al. Measurement of the t_{20} component of tensor analyzing power for the incoherent π^--meson photoproduction on a deuteron. *Nucl. Phys. A***1041**, 122781. https://doi.org/10.1016/j.nuclphysa.2023.122781 (2024).
25. Gauzshtein, V. et al. Measurement of the tensor analyzing power t_{20} for incoherent π^--photoproduction on a deuteron above the first resonance region. *Phys. Lett. B.***860**, 139166. https://doi.org/10.1016/j.physletb.2024.139166 (2025).
26. Iljinova, A. et al. Extension of the intranuclear cascade model for photonuclear reactions at energies up to 10 GeV. *Nucl. Phys. A***616**, 575. https://doi.org/10.1016/S0375-9474(96)00478-2 (1997).
27. Sober, D. I. et al. Bremsstrahlung tagged photon beam in Hall B at JLab. *Nucl. Instrm. Methods A***440**, 263. https://doi.org/10.1016/S0168-9002(99)00784-6 (2000).
28. Anthony, I., Kellie, J., Hall, S., Miller, G. & Ahrens, J. Design of a tagged photon spectrometer for use with the Mainz 840 MeV microtron. *Nucl. Instrm. Methods A***301**, 230. https://doi.org/10.1016/0168-9002(91)90464-2 (1991).
29. Shestakov, Y. et al. Tagging system for almost-real photons at VEPP-3 storage ring. *Phys. Part. Nucl.***45**, 338. https://doi.org/10.1134/S1063779614010924 (2014).
30. Dyug, M. et al. Internal polarized deuterium target with cryogenic atomic beam source. *Nucl. Instrm. Methods A***495**, 8. https://doi.org/10.1016/S0168-9002(02)01572-3 (2002).
31. Dyug, M. et al. Deuterium target polarimeter at the VEPP-3 storage ring. *Nucl. Instrum. Methods A***536**, 344. https://doi.org/10.1016/j.nima.2004.08.096 (2005).
32. Rose, E. M. *Elementary Theory of Angular Momentum* (Wiley, 1957).
33. Loginov, A., Sidorov, A. & Stibunov, V. Effect of rescattering on polarization observables of the reaction $\gamma d \to pp\pi^-$ in the delta-resonance region. *Phys. Atom. Nucl.***63**, 391. https://doi.org/10.1134/1.855646 (2000).
34. Kopylov, G. A model for the process of multiple production. *JETP***8**, 996 (1959).
35. Dalitz, R. & Yennie, D. Pion production in electron–proton collisions. *Phys. Rev.***105**, 1598. https://doi.org/10.1103/PhysRev.105.1598 (1957).
36. Haidenbauer, J. & Plessas, W. Separable representation of the Paris nucleon-nucleon potential. *Phys. Rev. C***30**, 1822. https://doi.org/10.1103/PhysRevC.30.1822 (1984).
37. Haidenbauer, J. & Plessas, W. Modified separable representation of the Paris nucleon–nucleon potential in the S-01 and P-03 states. *Phys. Rev. C***32**, 1424. https://doi.org/10.1103/PhysRevC.32.1424 (1985).
38. Fix, A. & Arenhövel, H. Three-body calculation of incoherent π^0 photoproduction on a deuteron. *Phys. Rev. C***100**, 034003. https://doi.org/10.1103/PhysRevC.100.034003 (2019).

Acknowledgement

The authors thank anonymous reviewers for useful comments and questions which helped to improve the paper.

Author contributions

Investigation: V.G., A.F., E.D., A.L., D.E., M.L. Data curation: V.I., D.N., I.R., Yu.S., D.T., B.V., A.Yu., S.Z., G.B., A.B., V.B., D.D., V.D., A.Z., K.K., A.K., V.K., E.L., I.L., T.M., R.M., I.M., I.O., P.P., L.S., E.S., S.S., M.S., E.S., I.U. Writing: V.G., A.F., E.D., A.L., I.R., D.T. Critical revision: D.N., Yu.Sh., H.A-E., S.Z. Final approval: all authors. All authors have read and agreed to the published version of the manuscript.

Funding

The data analysis part of this work was supported by TPU development program Priority 2030.

Declarations

Competing interests

The authors declare no competing interests.

Additional information

Correspondence and requests for materials should be addressed to V.G.

Reprints and permissions information is available at www.nature.com/reprints.

Publisher's note Springer Nature remains neutral with regard to jurisdictional claims in published maps and institutional affiliations.